Analytical study on effects of fracture energy and damping ratio on crack propagation in arch dams during large earthquakes

H. Sato, M. Kondo & T. Sasaki
National Institute for Land and Infrastructure Management, Ibaraki, Japan

ABSTRACT:

In the seismic performance evaluation of concrete dams against large earthquakes, crack propagation analysis based on smeared crack model is sometimes conducted to estimate the damage process and damaged areas. Various parameters must be set appropriately such as damping ratio and fracture energy for the analysis. However, it is frequently difficult to set the damping ratio, because it needs to be identified from strong motion records, and these have not been obtained in many dams. It is also difficult to set the fracture energy due to lack of experimental data for dam concrete. Therefore, in this paper, we have investigated the effects of fracture energy and damping ratio on the results of crack propagation analysis, using a Finite Element (FE) model of 3-D concrete arch dam. The results show the damping ratio has an important influence on crack distributions, and cracks in the dam body tend to decrease as the damping ratio increases. The results also show crack distributions in dam body are localized as the fracture energy increases.

1 INTRODUCTION

To evaluate seismic performance of arch dams during large earthquakes, crack propagation analysis is sometimes conducted, and it is necessary to appropriately set various parameters to accurately estimate damaged area. However, in some cases, it is not easy to appropriately set some parameters such as damping ratio when the strong acceleration record has not been obtained at the dam. It is also difficult to set the value of fracture energy because there are few test cases for dam concrete. Therefore, in this paper, for the purpose of grasping fundamental effects of fracture energy and damping ratio, basic analytical investigation was conducted on the influence of the fracture energy and damping ratio on the crack propagation analysis.

Fracture energy of dam concrete is an important parameter among the input physical properties required for evaluating crack growth of arch dams. The value is obtained from the fracture energy laboratory tests including wedge splitting tests, but there are few test cases for dam concrete using the maximum aggregate size of 80 to 150 mm. For this reason, we first conducted literature search to investigate the past experimental studies on the fracture energy obtained by the laboratory fracture energy tests using dam concrete of maximum aggregate size of 80 mm or more.

Damping ratio of an arch dam body is also an important parameter required for evaluating behavior of the dam during earthquakes. However, estimations of the damping ratio of arch dams during large earthquakes are often difficult because acceleration records with large Peak Ground Acceleration (PGA) have not been observed at arch dam sites. Although the number of observed records is limited, we estimate a damping ratio for analytical model during large earthquakes from the view point of the comparison of amplification ratios between observed and numerical results.

Then, we conducted crack propagation analyses based on the smeared crack model for an arch dam using 3-D FE model using three values of fracture energy and three values of damping ratio as input properties.

2 SUMMARY OF PREVIOUS TESTS ON FRACTURE ENERGY FOR DAM CONCRETE

A large number of experimental studies on the fracture behavior of concrete using relatively small aggregate have been conducted, but there are a few test cases of dam concrete using large aggregate. Literatures related to fracture energy tests satisfying the following conditions were gathered and organized.

1) Laboratory tests for dam concrete with maximum aggregate size, d_{max}, of 80 mm or more were conducted.
2) Relatively large fracture energy more than about 300 N/m was obtained.

A summary of the literature search results is shown in Table 1. The meaning of the symbols concerning the specimen size in Table 1 is shown in Figure 1. The results in Table 1 are summarized in order from the oldest published date. Some fracture energy test methods were proposed including a three point bending test and a wedge splitting test, but only the results of the wedge splitting test met the above two conditions in the literature search in this paper.

Table 1. Summary of fracture energy tests by wedge splitting tests for dam concrete.

Author(s)	Maximum aggregate size	Compres-sive strength	Tensile strength	Specimen size of wedge splliting test (mm)				H_2/d_{max}	Fracture energy		Specimen age for fracture energy test
	d_{max} (mm)	(N/mm^2)	(N/mm^2)	H_1	W	D	H_2		G_F (N/m)		
He et al. (1992)	76	16.92※2	2.00※2	1820	1820	230	1366	5.94	static	152	55 days
									rapid※8	1313	
Trunk et al. (1998)	125	-	-	3200	3200	-	1600	12.8	static	about 600	More than 1 year
Horii et al. (2000)	150	34.1※3	2.53※3	1200	1200	450	600	4	static	317	-
	20	17.6※4	1.84※4	200	200	100	100	5	rapid※9	349	-
Zhao et al. (2008)	80	51.7※5	-	1000	1000	500	500	6.25	static	about 660	1 year
Ishiguro (2014)	80※1	26.9※6	3.09※6	315	350	200	260	3.25	static	411	more than 91 days
Guan et al. (2015)	150	29.37※7	3.04※7	2250	2250	450	1350	9	static	759	180 days

*1: maximum aggregate size was 120 mm for mixing and specimens were prepared by wet screening using an 80 mm sieve, *2: specimen age is unknown, *3: specimen age is about 3 months, *4: specimen age is about 1 month, *5: specimen age is 1 year, *6: specimen age is 91 days, *7: specimen age is 180 days, *8: time to peak loading (130kN) is about 2.9 seconds, *9: CMOD velocity is 12400 cm/minute.

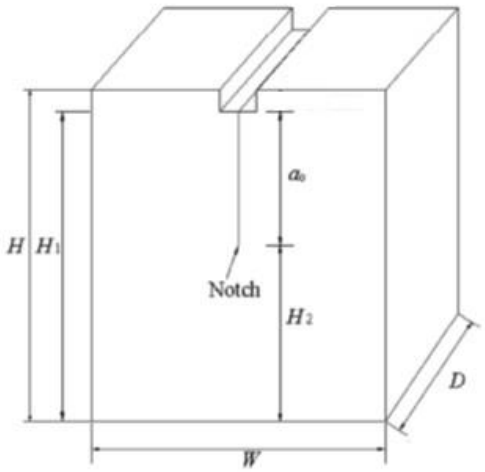

Figure 1. Outline of specimen used for wedge splitting tests.

He et al. (1992) conducted wedge splitting tests under the static and rapid loading conditions using specimens of d_{max} of 76 mm. In the rapid test condition, time to peak loading was about 2.9 seconds. Fracture energy values were 152 and 1313 N/m for static and rapid loading conditions respectively and the ratio of the fracture energy in rapid test result to that in the static condition was about 8.6 times.

Trunk et al. (1998) conducted wedge splitting tests using specimens of d_{max} of 125 mm. Specimen size was the largest and specimen age was the oldest in Table 1. Relatively large value of fracture energy of about 600 N/m was obtained by static loading test condition.

Horii et al. (2000) conducted wedge splitting tests under the static conditions using specimens of d_{max} of 150 mm and the fracture energy was 317 N/m. Horii et al. also conducted tests under the rapid loading conditions using specimens of d_{max} of 20 mm and the fracture energy was 349 N/m. Horii et al (2000) proposed the following approximate expression on fracture energy by the results in static loading condition.

$$G_F = (0.79d_{max} + 80) \times (f_c/10)^{0.7} \quad (1)$$

where G_F = fracture energy (N/m); d_{max} = maximum aggregate size (mm); and f_c = compressive strength (N/mm^2).

Zhao et al. (2008) conducted wedge splitting tests using specimens of d_{max} of 80 mm. Fracture energy tests were conducted at the age of one year of specimens. Relatively large value of fracture energy of about 660 N/m was obtained for static loading test condition.

Ishiguro (2014) conducted wedge splitting tests using relatively small specimens. Concrete used for tests was mixed using d_{max} of 120 mm and specimens (350 mm x 350 mm x 200 mm) were prepared by wet screening using an 80 mm sieve. Relatively large value of fracture energy of 411 N/m was obtained from static loading test condition.

Guan et al. (2015) conducted wedge splitting tests using relatively large specimens. Dam concrete mixed at an arch dam construction site was used. D_{max} was 150 mm and specimens were prepared by site-casting. Relatively large value of fracture energy of 759 N/m was obtained from static loading test condition. Guan et al. (2015) proposed the following approximate expression on fracture energy by the test results.

$$G_F = (0.1616d_{max} + 1.0263) \times f_c \quad (2)$$

where G_F = fracture energy (N/m); d_{max} = maximum aggregate size (mm); and f_c = compressive strength (N/mm^2).

Figure 2 shows fracture energies estimated by equations (1) and (2) when maximum aggregate size, d_{max}, is 150 mm. In Figure 2, the values of fracture energy are almost same when f_c is less than 10 N/mm^2, but the difference becomes larger as f_c increases. One of the reasons of the difference between the values of fracture energy in Figure 2 was thought to be a relatively small value of H_2/d_{max} in the test conditions of Horii et al. (2000) in Table 1. Many papers indicate that the values of H_2/d_{max} are important to obtain constant values of fracture energy independent from the maximum aggregate size in the laboratory wedge splitting tests. The values of fracture energy increase almost linearly to H_2/d_{max} when H_2/d_{max} is small, but the values of fracture energy become constant when H_2/d_{max} is larger than a threshold value. Guan et al. (2015) pointed that the threshold value of H_2/d_{max} was 6.

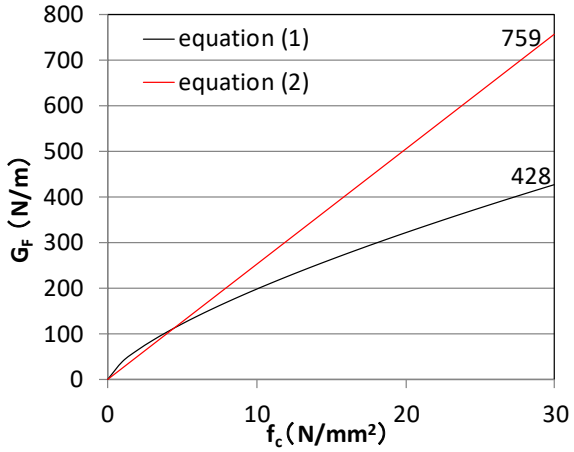

Figure 2. Relationship G_F and f_c of equations (1) and (2) in the case of d_{max} = 150 mm.

Based on the literature search results, three values of fracture energy were selected for crack propagation analysis to investigate the influences of the fracture energy on crack generation during earthquakes.

1) G_F = 428 N/m obtained by the equation (1) when f_c = 30 N/mm^2 and d_{max} = 150 mm shown in Figure 2. This value has sometimes been used for crack propagation analysis in Japan.
2) G_F = 759 N/m obtained by the test conducted by Guan et al. (2015) in the static loading test condition in Table 1. This value is also obtained by the equation (2) when f_c = 30 N/mm^2 and d_{max} = 150 mm shown in Figure 2.
3) G_F = 1313 N/m obtained by the test conducted by He et al. (1992) in the rapid loading test condition in Table 1.

3 ESTIMATION OF DAMPING RATIO OF ARCH DAMS DURING LARGE EARTHQUAKES

A damping ratio of a dam body can be estimated by the reproduction analysis using observed acceleration records at the dam site. However, estimations of the damping ratio of arch dams during large earthquakes are difficult because acceleration records with large PGA have not been obtained at many arch dam sites. Figure 3 shows a relationship between PGA in the upstream-downstream (UD) direction and amplification ratio of maximum accelerations at crest to PGA in UD direction based on observation records obtained at arch dams. The number of observation records in Figure 3 is limited, but the amplification ratio tends to decrease with PGA and the amplification ratio seems to be distributed from 5 to 10 when PGA is more than 1 m/s^2. Figure 4 shows a relationship between the damping ratio of the dam body and the amplification ratio of maximum accelerations at crest to PGA in UD direction using numerical results in this paper including both linear and nonlinear cases when input PGA is 3 m/s^2 in UD direction. In Figure 4, the amplification ratio tends to decrease with the damping ratio, and amplification ratios are distributed from 10 to 5 when damping ratios are 5 to 15 %.

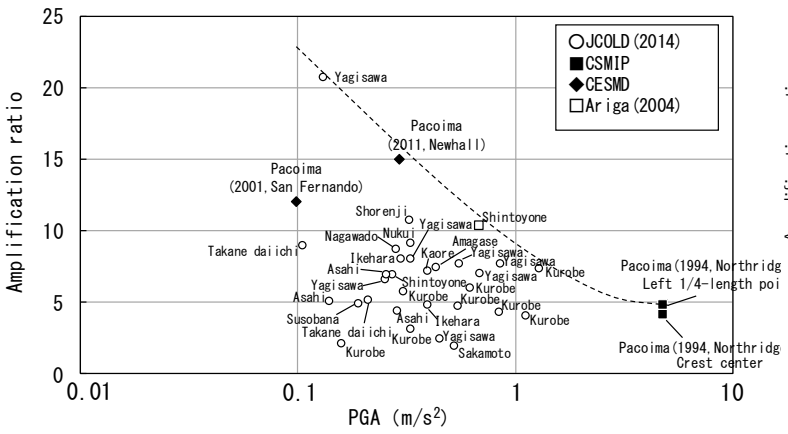

Figure 3. Relationship PGA and amplification ratio of observation records at arch dams. (after Sato, N., et al., 2013)

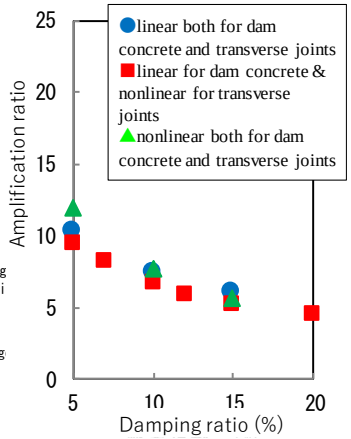

Figure 4. Relationship damping ratio and amplification ratio of analytical results using arch dam model in this paper when PGA is 3 m/s^2 in UD direction.

Based on considerations described above, three values of damping ratios, h, were selected for crack propagation analysis to investigate the influences of the damping ratio on cracks during large earthquakes.

1) h = 5 %, where amplification ratio is about 10 in Figure 4.
2) h = 10 %, where amplification ratio is about 7 in Figure 4.
3) h = 15 %, where amplification ratio is about 5 in Figure 4.

4 EFFECTS OF FRACTURE ENERGY ON CRACK PROPAGATION ANALYSIS FOR ARCH DAM

Embanking and impounding analysis were conducted to estimate initial stress. Then, dynamic analysis in the time domain and crack propagation analysis based on the smeared crack model were conducted to evaluate crack distributions during earthquakes according to fracture energy.

4.1 *Analytical model*

To investigate the influence of fracture energy on cracked area during earthquakes, crack propagation analysis based on the smeared crack model was carried out using a 3-D arch dam coupled model of dam body - foundation rock - reservoir (Figure 5). An arch dam model was used for study with a height and a water level of 105 and 93 meters, respectively. Reservoir was modeled by fluid elements and analyzed as a compressive fluid. Hexahedral elements with sides less than 1.5 m were used for dam body elements. The numbers of elements were 153,700, 70,448 and 149,392 for dam body, foundation rock and reservoir, respectively. The total number of elements was 373,540 for analysis. Transverse and peripheral joints were modeled using joint elements as shown in Figure 6, so that the opening and closing of the joint behavior can be considered in the analysis. The FE model software of ISCEF was used for analysis.

4.2 *Physical properties for analysis*

Physical properties used for analysis are shown in Table 2. Unit weight and tensile strength were obtained by the laboratory tests for dam concrete of the model dam. Elastic modulus of dam body and foundation rock were estimated by the reproduction analysis using observed small seismic records of the model dam. Poisson's ratio and damping ratio of dam body and foundation rock were the values generally used in seismic analysis for arch dams. To investigate the effects of fracture energy on crack propagation, three values of fracture energy were selected based on the literature research described in Chapter 2. For tension softening curve of dam concrete for crack propagation analysis, a linear function shown in Figure 7 was used.

Joint elements were used for the transverse and the peripheral joints so that the opening and closing of the joint behavior can be considered in the analysis. Physical properties for joint elements in Figure 8 were determined based on Nishiuchi et al. (2006) and Ariga et al. (2004).

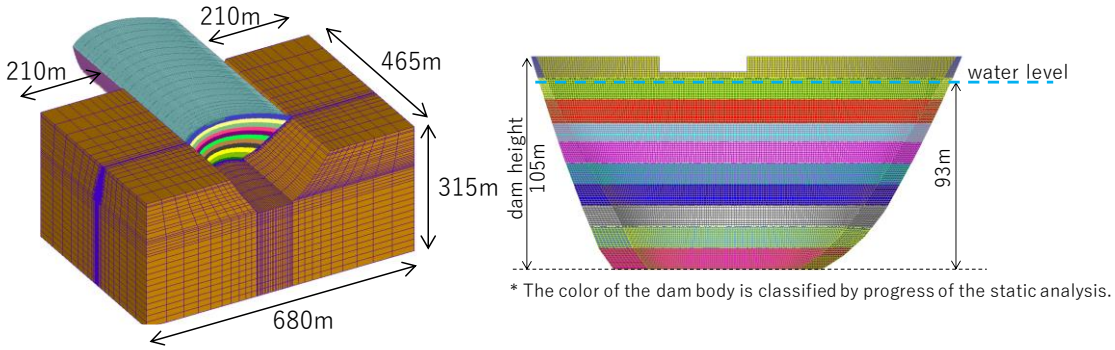

Figure 5. Entire analytical model (left) and downstream surface of dam body (right).

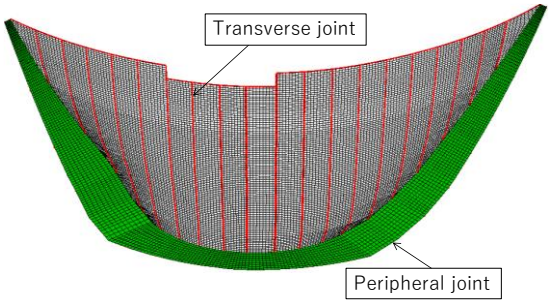

Figure 6. Transverse and peripheral joints.

Table 2. Physical properties for study.

	Unit weight (kN/m^3)	Elastic modulus (N/mm^2)	Poisson's ratio	Tensile strength (N/mm^2)	Fracture energy (N/m)	Damping ratio (%)
dam body	24.5	45600	0.2	3.3	428, 759, 1313	5, 10, 15
foundation rock	26.5	32500	0.25	-	-	5
reservoir	9.8	Compressible fluid (c=1472m/s)				

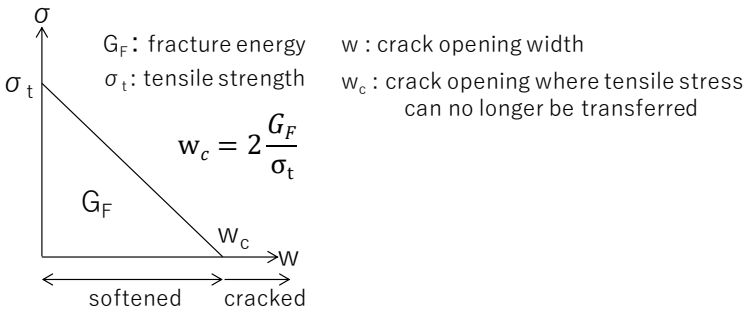

Figure 7. Tension softening curve used for analysis.

	Transverse joint element	Peripheral joint element
Axial modulus	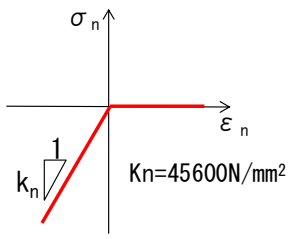	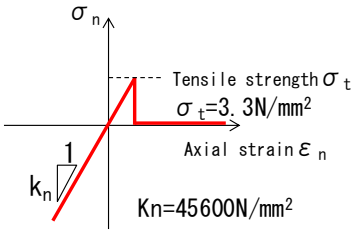
Shear modulus	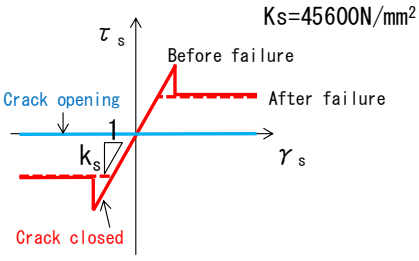	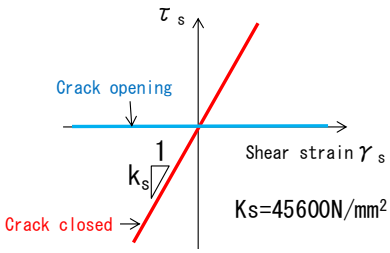
Damping ratio	1%	10%

Figure 8. Axial and shear modulus and damping ratio for transverse and peripheral joint elements.

4.3 *Input motions*

Figure 9 shows acceleration time histories and acceleration response spectrum of input motions for three directions when the PGA is 3 m/s^2 in UD direction. The original acceleration time history records were the records observed at the Kasho dam during the Western Tottori prefecture earthquake in 2000 and the records were arranged for input motions by amplitude adjustment and spectrum fitting to the target acceleration and the target spectrum. Figure 9 also shows minimum acceleration response spectrum in Japanese guidelines (River bureau of MLIT, 2005), and the acceleration response spectrum of the input acceleration used for the analysis was set to conform to Japanese guidelines as shown in Figure 9. In order to shorten the time required for numerical analysis, acceleration time histories from 7 to 14 seconds with relatively large accelerations were used as shown in Figure 9.

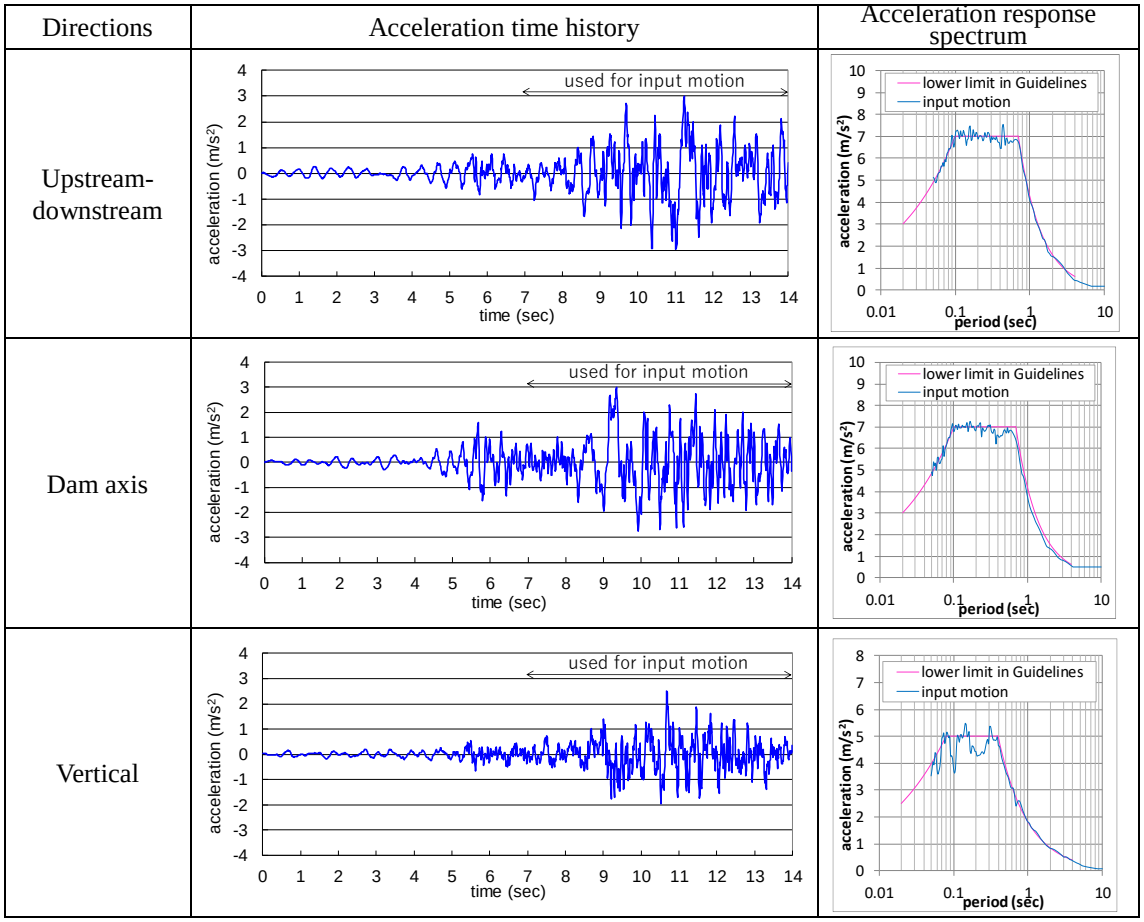

Figure 9. Acceleration time histories and acceleration response spectrum of input motions in the case of the maximum acceleration of 3 m/s^2 in UD direction.

4.4 *Analysis results*

Figure 10 shows openings of transverse joint elements using input motions with the PGA of 3 m/s^2 in the UD direction. Red joints mean that the joint elements have opened. Many joints have opened in Figure 10. As the damping ratio increases, the number of opened joint elements decreases, especially in the mid-part of dam body. It seems that joint opening area has something to do with damping ratio, but less to do with fracture energy.

Figures 11 and 12 show the results of cracked and softened elements distributions in the upstream and downstream surfaces, respectively, using input motions with the PGA of 3 m/s^2 in the UD direction. In the figures, red elements show cracked area, and yellow elements show softened area where the tensile stress exceeds the tensile strength but a crack is not penetrated in the element. In Figure 11, cracked or softened elements in the upstream surface are confirmed only in the case of damping ratio of 5 %. In the case of damping ratio of 5 % and fracture energy of 428 N/m in Figure 11, some vertical cracks from the crest and several horizontal cracks are confirmed. In the case of damping ratio of 5 % and fracture energy of 759 N/m in Figure 11, several vertical cracks from the crest are confirmed, but no horizontal cracks are confirmed. In the case of damping ratio of 5 % and fracture energy of 1313 N/m in Figure 11, no cracked elements are confirmed, and only some softened elements are confirmed. When the damping ratio is 10 % or 15 %, no cracked or softened elements are confirmed in Figure 11, because increasing the damping ratio reduces the response of the dam body.

The number of cracked or softened elements in downstream surface of dam body in Figure 12 is larger than that in upstream surface in Figure 11. In the case of damping ratio of 5 % in Figure 12, a lot of cracked or softened elements are confirmed, and the number of cracked elements is decreasing but that of softened elements is increasing as the fracture energy increases. The results also show crack distributions in dam body are localized as the fracture energy increases.

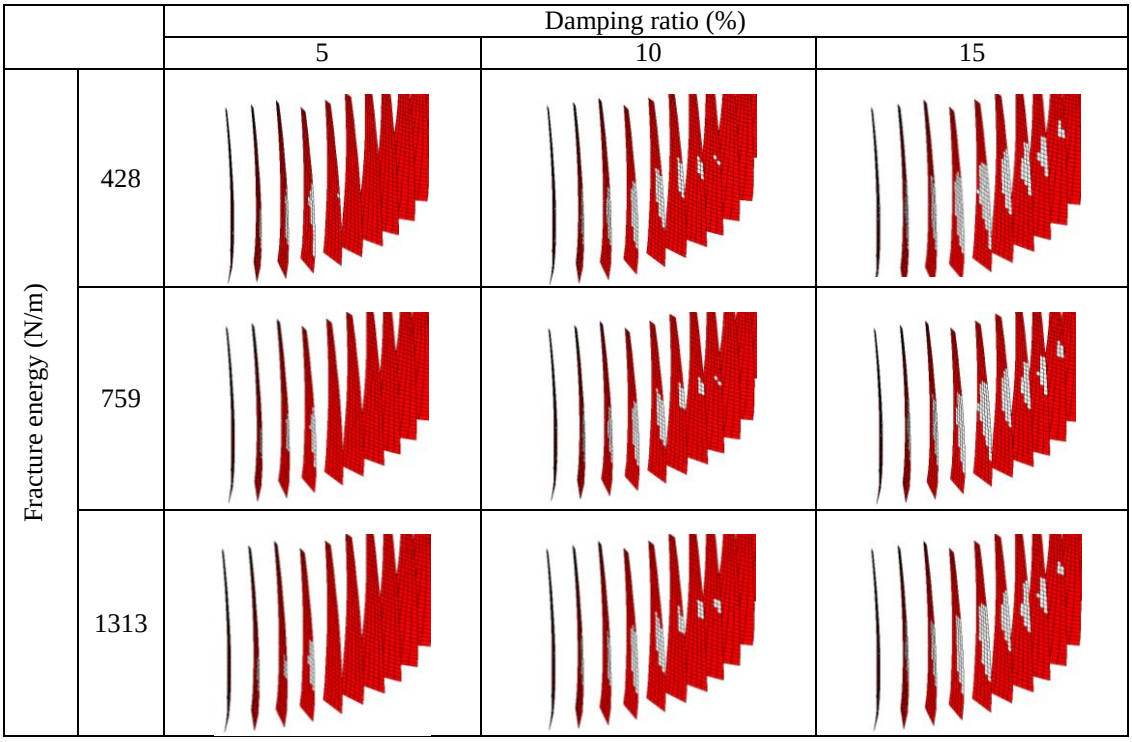

Figure 10. Openings of transverse joint elements near crown in the case of the maximum acceleration of 3 m/s^2 in UD. (Red : opened)

This is because that softened elements relatively immediately become cracked elements in a small fracture energy of 428 N/m, but softened elements do not soon become cracked elements because of a large fracture energy of 1313. In other words, cracked elements cannot transmit tensile stress, but softened elements can transmit tensile stress so that relatively large tensile stress more than tensile strength are generated around previously softened elements. In Figure 12, in the cases of the damping ratios of 10 and 15 %, same tendency is confirmed that the number of cracked elements is decreasing but that of softened elements is increasing as the fracture energy increases. In the case of the damping ratio of 10 %, several horizontal cracked elements are confirmed in the case of fracture energy of 428 N/m, but no cracked elements and some softened elements are confirmed in the case of fracture energy of 1313 N/m. In the case of the damping ratio of 15 %, the number of cracked or softened elements is smaller than that in the case of the damping ratio of 10% and only softened elements are confirmed in the case of fracture energy of 759 and 1313 N/m.

According to above considerations, increasing of the damping ratio has influences on the decreasing of cracked and softened elements and on the decreasing of opened joint elements, because increasing of the damping ratio reduces the response of the dam body. Increasing of the fracture energy has influences on the decreasing of cracked elements but the increasing of softened elements. Main differences of the effects of the damping ratio and the fracture energy is that the increasing of the damping ratio leads to the decreasing of softened elements but the increasing of the fracture energy leads to the increasing of softened elements.

If we want to know the value of the damping ratio for large earthquakes, we must wait for the occurrence of a large earthquake and then evaluate a damping ratio by reproduction analysis, but it is difficult to evaluate the damping ratio accurately because large earthquake rarely occurs. Determination of the fracture energy seems easier because we can evaluate a fracture energy by an appropriate laboratory test. For evaluation of the damping ratio during large earthquakes it is important to continue to observe and collect seismic records in the future. For evaluation of the fracture energy of arch dams, more laboratory tests are needed using dam concrete with more large compression strength using large aggregate.

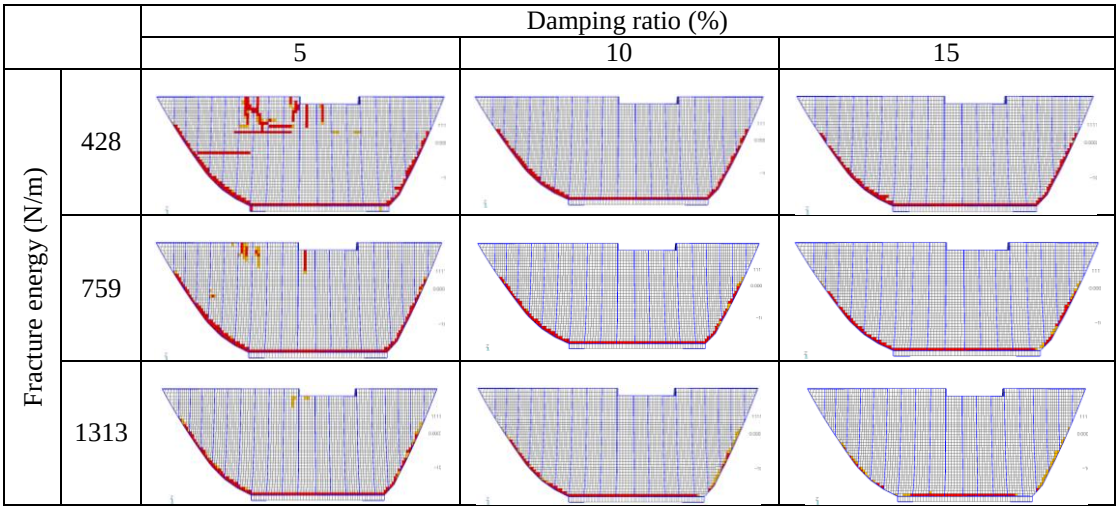

Figure 11. Cracked and softened element distributions of upstream surface in the case of the maximum acceleration of 3 m/s^2 in UD direction. (Red : cracked, yellow : softened)

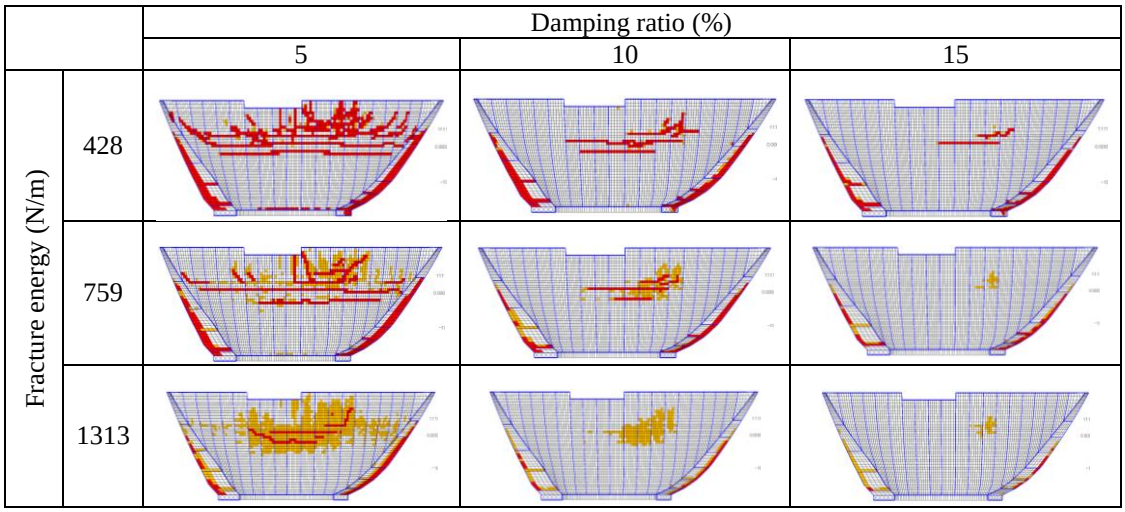

Figure 12. Cracked and softened element distributions of downstream surface in the case of the maximum acceleration of 3 m/s^2 in UD direction. (Red : cracked, yellow : softened)

5 CONCLUSIONS

To investigate the effects of fracture energy and damping ratio on the crack propagation in an arch dam during large earthquakes, a literature search was conducted to evaluate the fracture energy of dam concrete and an estimation of damping ratio during large earthquakes was tried from the view point of the amplification ratio. Then, crack propagation analyses were conducted and the following conclusions were obtained.

1) We investigated the past experimental studies on the fracture energy laboratory tests. Literatures related to fracture energy tests satisfying the following conditions were gathered. First condition was that laboratory tests for dam concrete with maximum aggregate size of 80 mm or more were conducted. Second condition was that relatively large fracture energy more than about 300 N/m was obtained. We found six papers satisfying the conditions and summarized test conditions and test results. Relatively large values of fracture energy were obtained by the tests in the papers and the maximum values were 759 and 1313 N/m by static and rapid loading conditions, respectively. These values are only the results of the literature search in this paper, so it is possible larger fracture energy has been obtained in other papers.
2) Although there were small number of observed acceleration time history data obtained at the arch dam sites, the amplification ratios of the observed data tended to decrease as the PGA

increased. The amplification ratios were distributed from 5 to 10 when PGA was 1 m/s^2 or more, and amplification ratios in the analytical model of this paper using 3 m/s^2 of PGA were distributed from 5 to 10 when the damping ratios were 5% to 15%.

3) Crack propagation analyses based on the smeared crack model for an arch dam with a height of 105 m using 3-D FE model were conducted. Joints were modeled by the joint elements to reproduce nonlinear behavior of the joints of the arch dam. The time history with maximum accelerations of 3 m/s^2 was used for input motions. The input values of three fracture energies were determined based on the literature search and the input values of three damping ratios were determined from the view point of the amplification ratio. The numerical results showed that both fracture energy and damping ratio had important influences on crack distributions. As fracture energy increased, cracked area in downstream surface of the dam body became smaller and cracks were localized, but softened area became larger. As damping ratio increased, both cracked and softened area in dam body became smaller because increasing the damping ratio reduced the response of the dam body. We think fracture energy of dam concrete is larger than the values used for the analysis in this paper, because there have been no cases of cracks in six arch dam body that experienced observed or estimated PGA of 3 m/s^2 or more. (Nuss et al, 2012)

PREFERENCES

Ariga, Y., Cao, Z. and Watanabe, H. 2004. Study on 3-D dynamic analysis of arch dam against strong earthquake motion considering discontinuous behavior of joints. *Journal of Japan Society of Civil Engineers*: 759: 53-67. (in Japanese)

CESMD (Center for Engineering Strong Motion Data), https://www.strongmotioncenter.org/.

CSMIP (California Strong Motion Instrumentation Program). 1994. Strong-Motion Records from the Northridge, California Earthquake of January 17, 1994, Report No. OSMS 94-07.

Guan, J., Li, Q., Wu, Z., Zhao, S., Dong, W. and Zhou, S. 2015. Minimum specimen size for fracture parameters of site-casting dam concrete. *Construction and Building Materials*: 93: 973-982.

He, S., Plesha, M., Rowlands, R. and Bezant, Z. 1992. Fracture energy tests of dam concrete with rate and size effects. *Dam Engineering*: III: 139-159.

Horii, H., Uchita, Y., Kashiwayanagi, M., Kimata, H. and Okada, T. 2000. Study on tensile softening characteristics for evaluating concrete dam strength. *Electric Power Civil Engineering*: 286: 113-119. (in Japanese)

ISCEF. http://www.century-techno.co.jp/products/.

Ishiguro, S. 2014. Wedge splitting tests of concrete with large coarse aggregate size. *Proceedings of the Japan Concrete Institute*: 36: 1: 352-357. (in Japanese)

Nishiuchi, T. and Sakata, K. 2006. Investigation on static behavior of existing arch dams using finite element method considering nonlinear behavior of transverse joints. *Journal of Japan Society of Civil Engineers*: 62: 4: 672-688. (in Japanese)

Nuss, L. K., Matsumoto, N. and Hansen, K., D. 2017. Shaken, but not stirred - earthquake performance of concrete dams, *Presentation from USSD Conference, New Orlrans*, http://www.ussdams.org/wp-content/uploads/2016/05/Session1_Case-Histories-and-Seismic-PFM.pdf.

River Bureau, Ministry Land, Infrastructure, Transport and Tourism (MLIT), 2005. Guidelines for seismic performance evaluation of dams during large earthquakes (draft).

Sato, N., Soda, H. and Ootagaki, K. 2013. Estimation of dynamic characteristics and physical properties of dams based on observed earthquake records, *Engineering for dams*, 321: 40-47. (in Japanese)

Trunk, B. and Wittmann, F.H. 1998. Experimental Investigation into the Size Dependence of Fracture Mechanics Parameters. *FraMCoS-3*: 1937-1948. Gifu.

Zhao, Z., Kwon, S. and Shah, S. 2008. Effect of specimen size on fracture energy and softening curve of concrete: Part I. Experiments and fracture energy. *Cement and Concrete Research*: 38: 1049-1060.